Hindawi
Geofluids
Volume 2019, Article ID 2374236, 16 pages
https://doi.org/10.1155/2019/2374236

Research Article

The Impact of Reservoir Fluctuations on Reactivated Large Landslides: A Case Study

Javed Iqbal,[1,2] **Xinbin Tu**,[2,3] **and Wei Gao**[2]

[1]*Key Laboratory for Mountain Hazards and Earth Surface Process, Institute of Mountain Hazards & Environment, Chinese Academy of Sciences, Chengdu, China*
[2]*Institute of Geology and Geophysics, Chinese Academy of Sciences, Beijing 100029, China*
[3]*State Grid Corporation of China, Beijing 100031, China*

Correspondence should be addressed to Javed Iqbal; javediqbalgeo@gmail.com and Wei Gao; gaowei@mail.iggcas.ac.cn

Received 18 September 2018; Revised 11 January 2019; Accepted 27 February 2019; Published 15 April 2019

Guest Editor: Roberto Valentino

Filling of Xiangjiaba Reservoir Lake in the Southwest China triggered and reactivated numerous landslides due to water fluctuation. In order to understand the relationship between reservoirs and slope instability, a typical reservoir landslide (Dasha landslide) at the right bank of Jinsha River was selected as a case study for in-depth investigations. The detailed field investigations were carried out to identify the landslide with respect to its surroundings and to find out the slip surface. Boreholes were drilled to find out the subsurface lithology and the depth of failure of Dasha landslide. The in situ geotechnical tests were performed, and the soil samples from exposed slip surface were retrieved for geotechnical laboratory analysis. Finally, stability analysis was done using the 3D strength reduction method under different conditions of reservoir water level fluctuations and rainfall conditions. The in-depth investigations show that the Dasha landslide is a bedding rockslide which was once activated in 1986. The topography of Dasha landslide is relatively flat, while the back scarp and local terrain is relatively steep. The total volume of landslides is about 580×10^4 m^3 with an average thickness of 20 m. Bedrock in the landslide area is composed of Suining Formation of the Jurassic age. The main rock type is silty mudstone with sandstone, and the bedding orientation is 300~310° ∠ 7~22°. The factor of safety (FOS) of Dasha landslide obtained by 3D strength reduction cannot meet the minimum safety requirement under the working condition of reservoir level fluctuation as designed, with effect of rainfall and rapid drawdown.

1. Introduction

Landslides are common natural hazards which include a wide range of ground movement, such as rockfalls, deep failure of slopes, and shallow debris flows, which can occur in offshore, coastal, and onshore environments. Although gravity is the primary driving force for a landslide to occur, there are other contributing factors affecting the original slope stability.

Various studies have been done on reservoir slopes; however, there are two common factors which are always taken into consideration which include the effect of reservoir water on the slope and the corresponding effect of landslide on reservoir if slope fails. Particular considerations include the following: (i) reservoir slopes are subjected to load changes as a result of inundation when the reservoir is filled and subsequently as a result of variations in lake level during operations, (ii) the reservoir impounding affects the slope material properties and generates more adverse groundwater conditions than previously existed within the slope, creating reservoir-specific changes that can lead to instability, and (iii) the reservoir can increase the probability and consequences of failure, which may include total or partial blockage of the reservoir, the possibility of damaging impulse waves which may have effects that extend beyond the reservoir [1].

Until 1963, the reservoir landslides were not studied in depth, and the first detailed studied landslide (Vaiont landslides in Italy) became the benchmark for reservoir slopes studies. It is found that maximum large reservoir landslides are the old reactivated landslides [1]. Maximum landslides

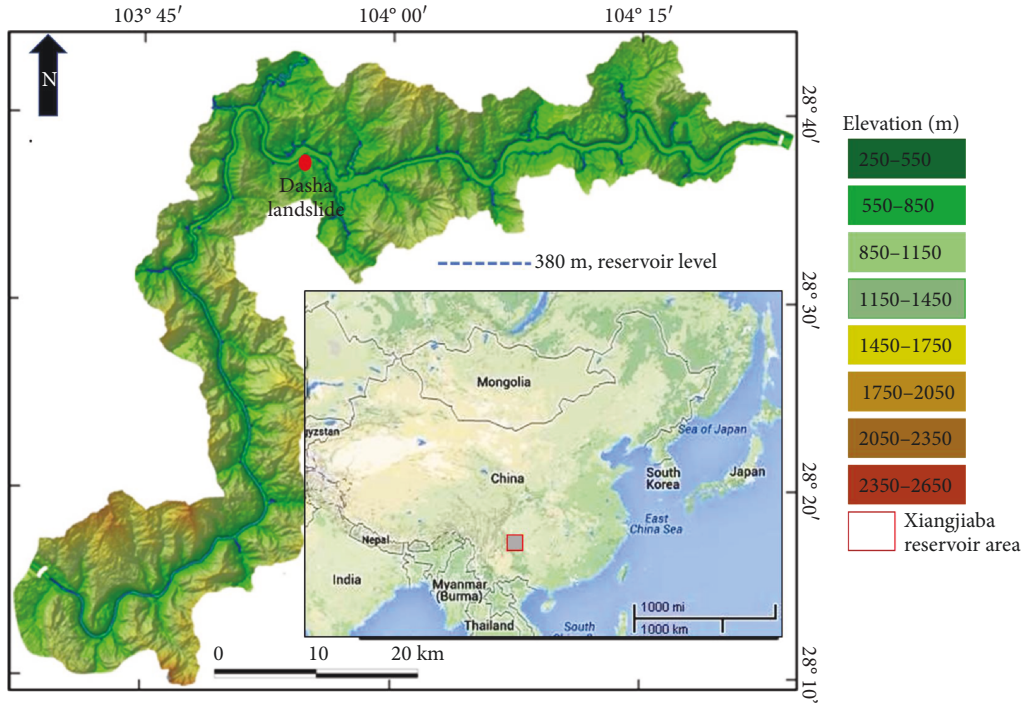

Figure 1: Topography of the reservoir area.

reactivate during the reservoir impoundment period or just after completion of the reservoir construction [2].

There are several studies found on Chinese reservoir landslides with different sets of objectives and outcomes (e.g., [3–13]). Various studies have been carried out in the Xiangjiaba reservoir area [14–16] and other reservoirs [17–20].

The impoundment of the Xiangjiaba reservoir is planned up to 380 m elevation in three stages. In the first stage, the reservoir filled to 354 m (October 12-16, 2012). In the second stage, the reservoir level increased to 370 m (June 26 to July 5, 2013). In the last stage, the reservoir reached to its maximum planned level of 380 m (September 7-12, 2013). Due to multiple episodes of reservoir rise and fall, the slopes were subjected to different conditions of alternate wetting and drying which may affect the stability of the slope. In addition, rainfall could also elevate the groundwater level which may create adverse effects on the stability of the slope. The current study is aimed at analyzing these impacts on the old reactivated large landslides.

2. Field Investigation and Landslide Descriptions

Dasha landslide is located at Dasha town, Suijiang County, at the right bank of Jinsha River about 60 km upstream of the Xiangjiaba damsite (Figures 1–3). In the northeast of the landslide near the Jinsha River, there is a about 260~370 m terrace, while in the southeast of the landslide there is also a flat terrace widely covered with alluvial deposits, between them there is a gully. Two bank slopes of the gully are quite different. The inclination of the bank slope with landside is low, while the river alluvial sediments terrace is very steep. In the north of the landslide, the red-bed hills are distributed along with alluvial sediments having gentle slope. In the west of landslide, a steep slope adjoins Gaofengshi Mountains, whose height is 687 m. Bedrock in the landslide area is composed of Suining Formation of the Jurassic age, which is composed of reddish brown or purple silty mudstone with sandstone interlayer; rock orientation is 300°~310° ∠ 7°~22°. These rocks are distributed in the steep slope area in the west (back edge) of the landslide and along the Jinsha River bank slope (along highway) in the north and gully bottom in the east.

It is revealed through drilling that the landslide slope is composed of clay, silt with some rock fragments, and the underlying bedrock orientation is 310°∠15°. This landslide was reactivated during the rainy season in 1986, resulting in structural damages to homes and the ground surface. There is mainly a paddy field on the landslide slope; on the edge of landslide, water permeates into the gulley; on the back margin of the landslide, obvious cracks can be observed in house walls (Figure 4). So, the rise of the ground water level as a result of rain in the landslide should be the main cause of the landslide deformation. Eliminating local terrain effect, the strike of tensional cracks is 315 to 340°, with inclination of 60 to 70°. According to the drilling data, bedrock orientation and the relationship with landslide directions of movement, landslide should be the creep deformation of the overlying loose deposits along the underlying bedrock. In the past decade, paddy field became upland dry land. During the current investigations, no groundwater infiltrated on the edge of landslide, and creep deformation of the landslide mass is not very obvious; so, the groundwater level change is the controlling factors of landslide deformation.

The overall topographic slope angle of the terrain is less than 15°; however, the head scarp and local terrain is

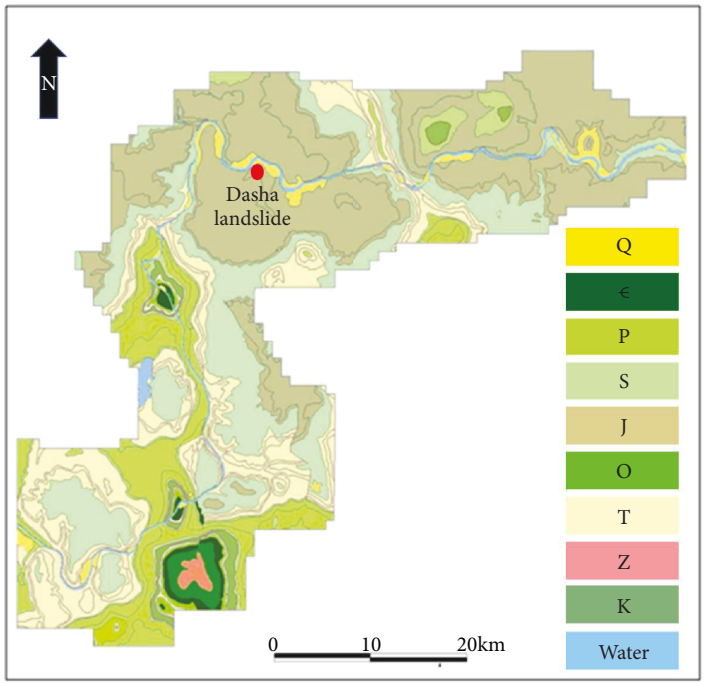

Figure 2: Generalized geological map of the Xiangjiaba reservoir area. Where Sinian system = Z; Cambrian system = Є; Ordovician system = O; Silurian system = S; Permian system = P; Triassic system = T; Jurassic system = J; Cretaceous system = K; Quaternary system = Q.

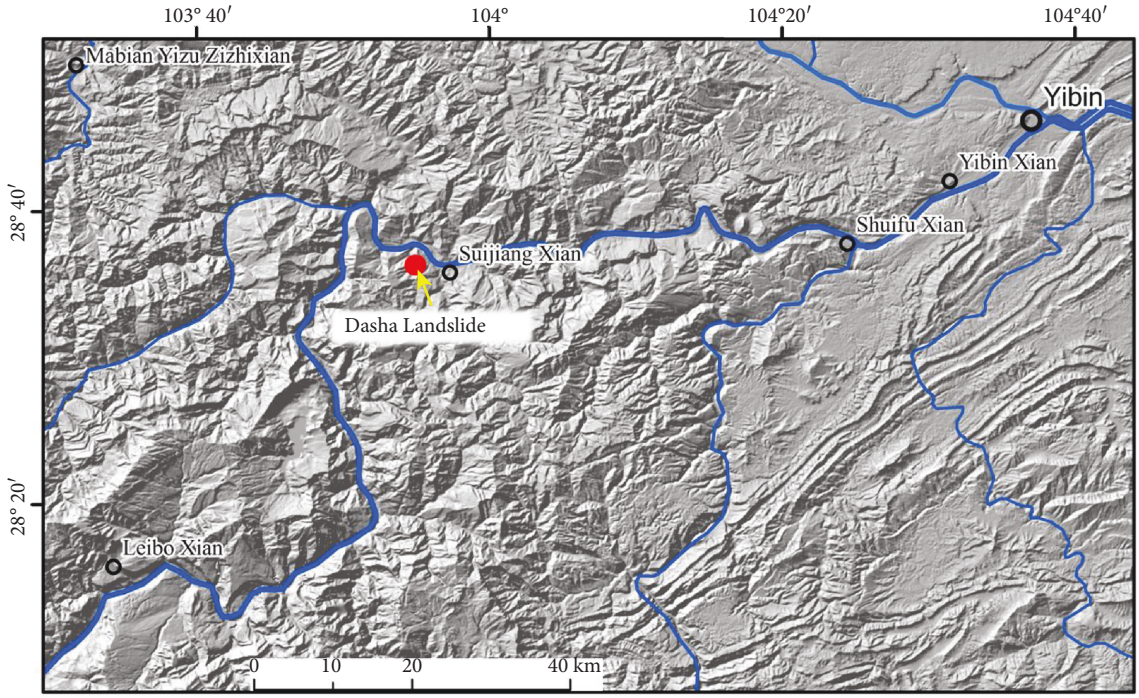

Figure 3: Location map of Dasha landslide.

relatively steep. The landslide area is about 29×10^4 m^2; the thickness of the landslide revealed by drilling is about 40 m, with the average thickness being about 20 m. The volume of the landslide is estimated to be about 580×10^4 m^3. From the landform conditions and air photo interpretation, a secondary landslide developed on the frontal margin of the landslide with clear chair-shaped landform is about 2.7×10^4 m^2 in area and about 16×10^4 m^3 in volume with the average thickness of about 6 m (Figures 5 and 6).

In the last decade, the paddy field was transformed into dry land, the groundwater levels lowered in the landslide, and the deformation of the landslide is not very obvious,

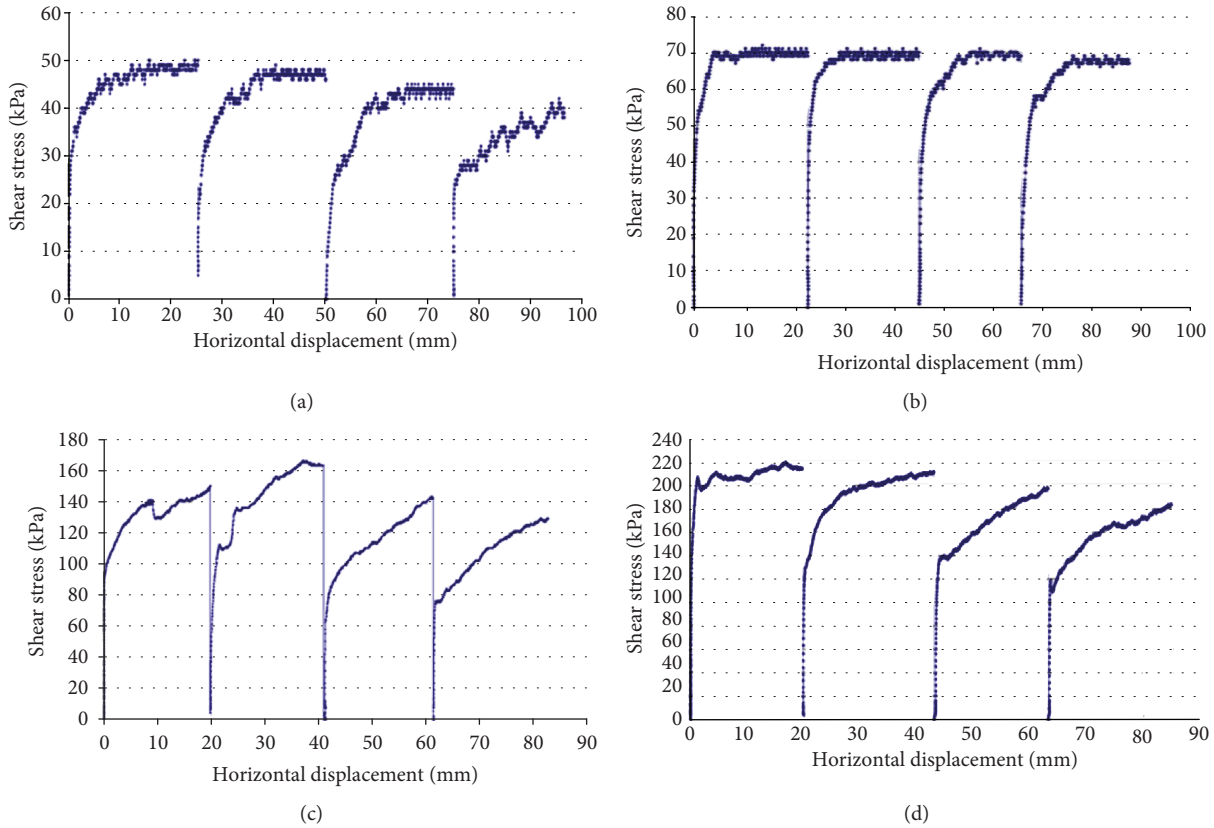

Figure 4: The shear stress-displacement curve of repeated direct shear at different normal stresses. (a) 60 kPa, (b) 110 kPa, (c) 260 kPa, and (d) 410 kPa.

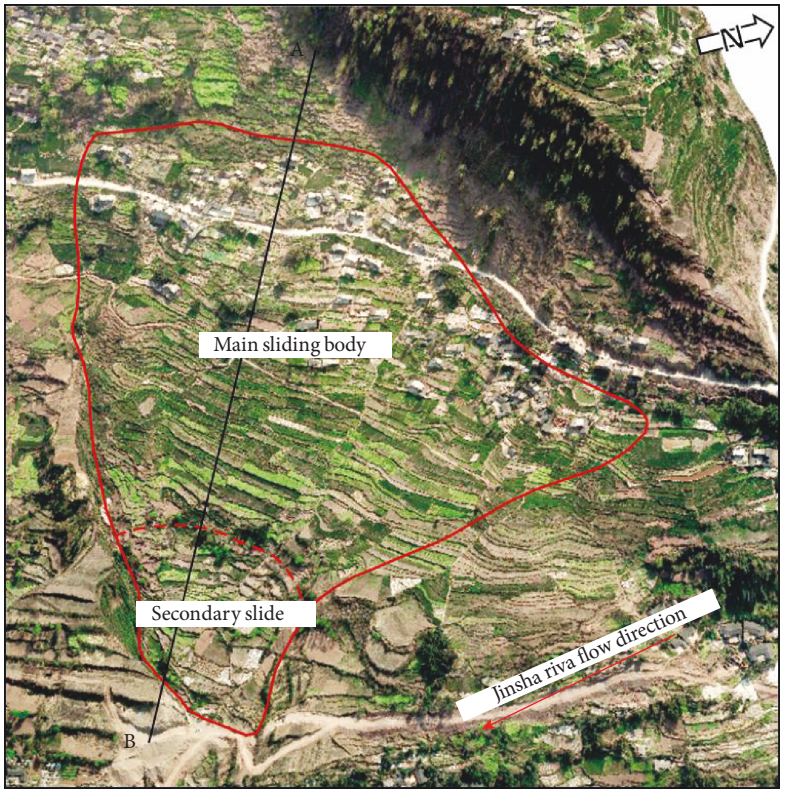

Figure 5: Remote-sensing image of Dasha landslide.

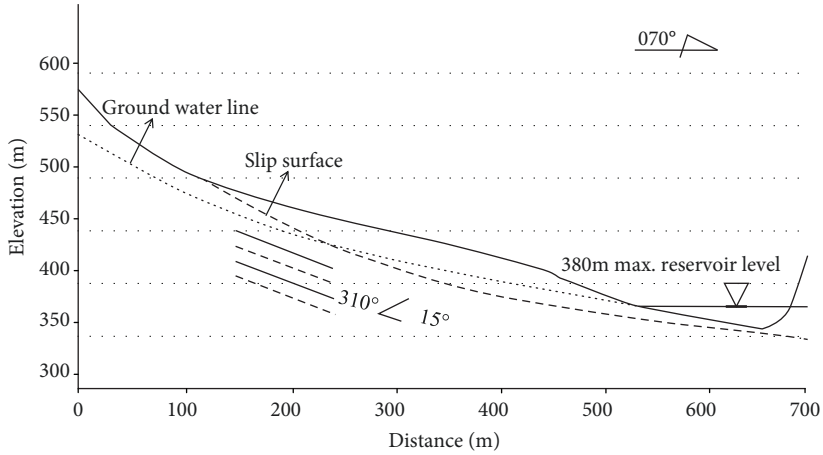

Figure 6: Cross-section of Dasha landslide (A-B).

(a) (b)

Figure 7: (a) A view of Dasha landslides; (b) tensional cracks in house wall.

but local visible cracks in the house wall can be found (Figure 7). This means that the landslide is still in the state of potential instability under the condition of the groundwater level rising or heavy rain. According to aerial photographs, houses are dense in the middle and back part of the landslide; hence, once the landslide moves perceptibly, it would create a huge loss in terms of human and property.

3. Geotechnical Laboratory Tests

Undisturbed soil samples taken near the slip surface were tested in the laboratory. Basic properties such as specific gravity, grain sizes, liquid limit, and plasticity index were measured. The natural density, dry density, and degree of saturation were found to be 2.233 g/cm^3, 1.975 g/cm^3, and 89%, respectively. The specific gravity was found to be 2.78 g/cm^3. The liquid limit, plastic limit, and plasticity index were found to be 25.8%, 19.7%, and 6.1, respectively. These basic properties were used in preparing the remolded samples for laboratory testing as well as in numerical simulation process to set the parameters. The laboratory direct shear tests are discussed below.

3.1. Medium-Sized Saturated Reversal Direct Shear Tests on Undisturbed Samples. The undisturbed samples were soaked for more than 24 hours. The size of the samples is 20 × 20 × 15 cm. The horizontal shear rate of direct shear apparatus that was used for the tests can be controlled by regulating the motor speed, and the shear rate was 2.2 mm/min (fast shear); it could be stopped when the maximum shear displacement reaches 20 mm. The vertical loading system of direct shear apparatus was hydraulic pressure, and the pressure sensor of the apparatus has low accuracy, so the values of normal stress were acquired by vertical pressure sensor during tests.

The actual values of normal stress are 61, 110, 260, and 410 kPa, and the shear strength after the forth cycles of shearing is considered the residual strength. The displacement of one-way shear is more than 20 mm, and the cumulative displacement would be more than 80 mm after four cycles of shearing. During the first shear, all of the four samples reached the peak quickly and kept the shear stress stable. However, it was different after the two or three times of shearing, and the shear stress tends to increase. The shear stress-displacement curves at different normal stresses are shown in Figure 4, and the first peak value of shear stress is peak strength. According to the first shear strength and the

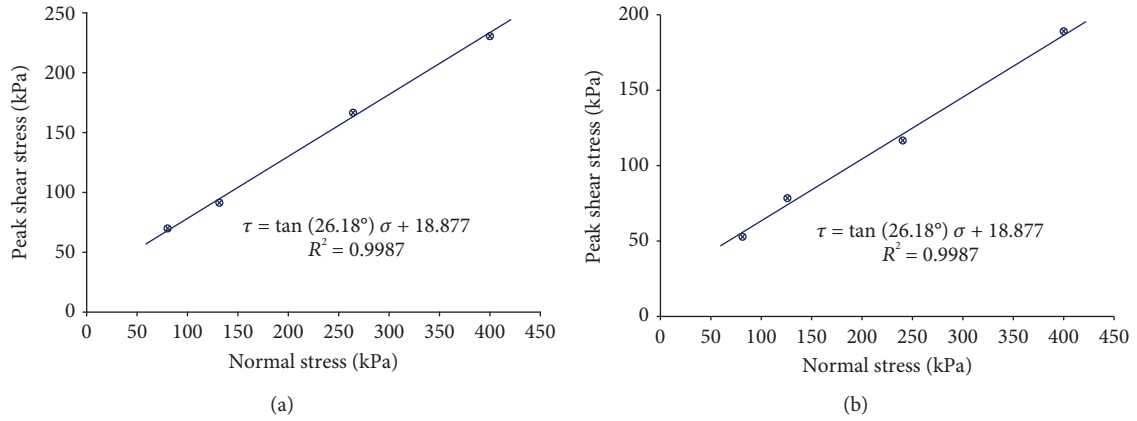

Figure 8: Graph showing the peak and residual strength parameters.

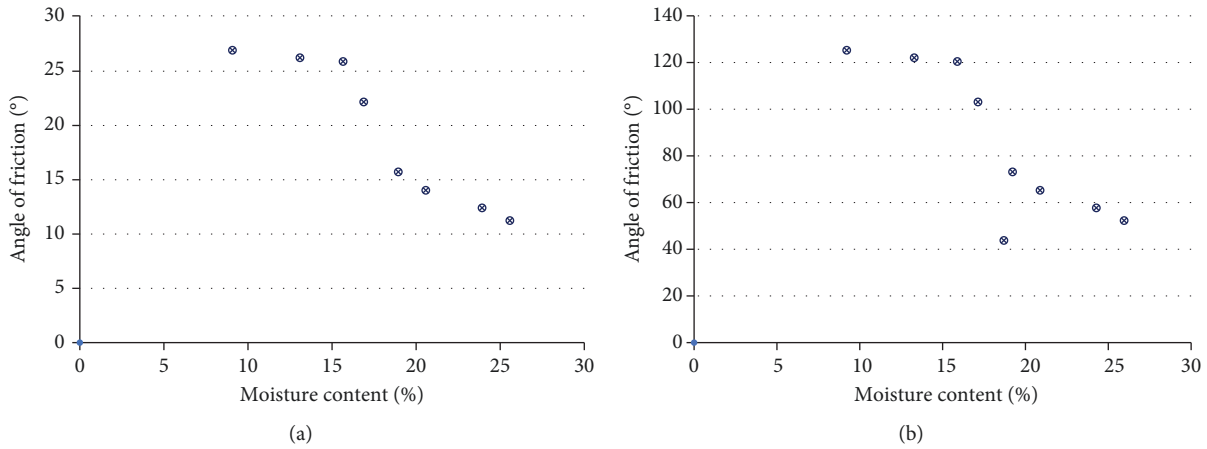

Figure 9: Effect of moisture on strength parameters.

last stable strength, the relationship between shear strength and normal stress can be drawn. As shown in Figure 8, the peak shear strength and the residual shear strength in the form of frictional angle and cohesion are 26.18°, 18.88 kPa and 21.38°, 17.95 kPa, respectively. The average moisture content of the soil samples measured from shear surface after opening of the shear box is 17.0%.

3.2. Medium-Size Direct Shear Test on Remolded Samples. Dasha landslide is a typical bedding landslide of red beds, and the particle size decreases with increase in depth. The soil samples consisting of high proportion of gravel-sized particles were taken near the toe of landslide at a depth of 1.5 m. The soil samples were remolded and prepared with different moisture content in order to explore the relationship between soil strength of the slope and water content. The size of samples is $20 \times 20 \times 15$ cm, and the shear rate is 1.0 mm/min. Under the consolidated and drained conditions, seven groups (each group with three samples) were tested in this series, and the moisture content of each group was determined after each test (Figures 9 and 10). As shown in Table 1, the direct shear tests for the soil with less than 2 mm particle size, the strength parameters are greatly influenced by the moisture content, and with a decrease in moisture content, the angle of friction and cohesion increases.

3.3. The Triaxial Consolidation Undrained Shear Tests. Three triaxial shear tests for Dasha landslide were performed in consolidated-undrained condition. The results of shear tests are shown in Figure 11. The effective cohesion and angle of friction for groups A, B, and C are 11.4 kPa and 22.5°, 21.6 kPa and 24.1°, and 23.4 kPa and 25.2°, respectively (Figure 11 and Table 2). It is observed that the shear strength parameters including cohesion and angle of internal friction of all three groups (A, B, and C) are in very small range, showing the reliability of the results which were later used in the simulation process.

4. Geotechnical In Situ Tests

The test was done on soil samples located near the toe of the landslide (fine sand and clay). The direct shear models were built on bedrock, which were perpendicular to the surface of bedrock, and specimens were pushed to shear along the bedrock. Two groups of large-sized direct shear tests (sample size of $50 \times 50 \times 40$ cm) were carried out at this test site to compare and better understand the results of in situ tests. The predefined values of normal stress were 50 kPa, 100 kPa, 150 kPa, and 200 kPa, and there was some deviation between the measured values and the predefined values of normal stress. Therefore, for the fitting of strength parameter

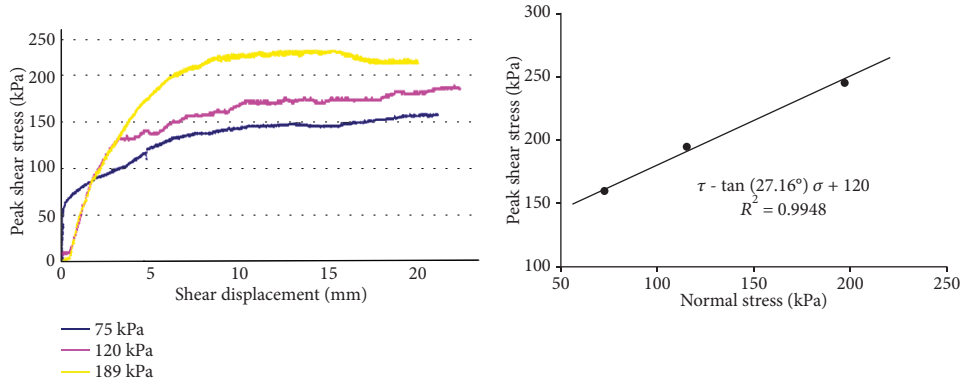

(a)

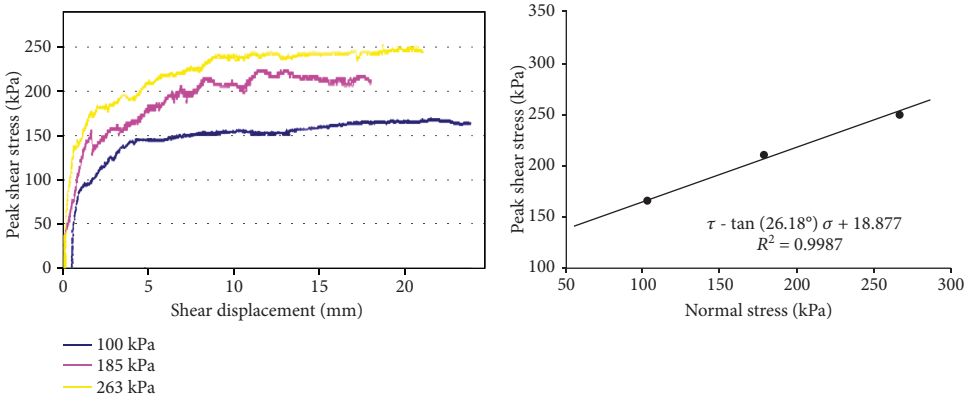

(b)

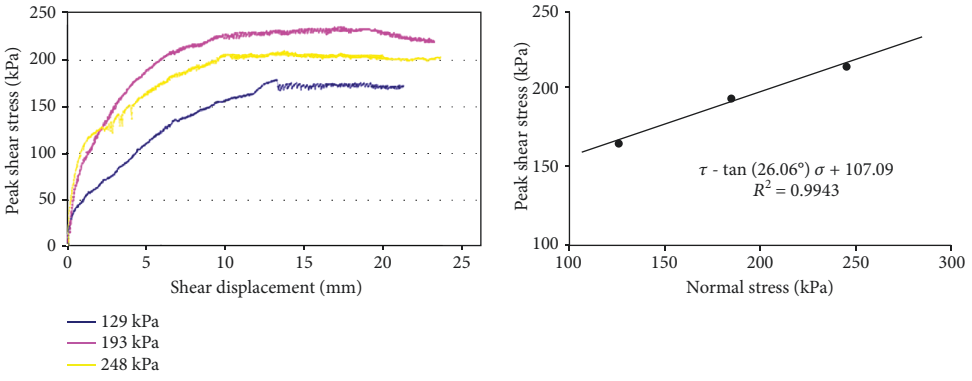

(c)

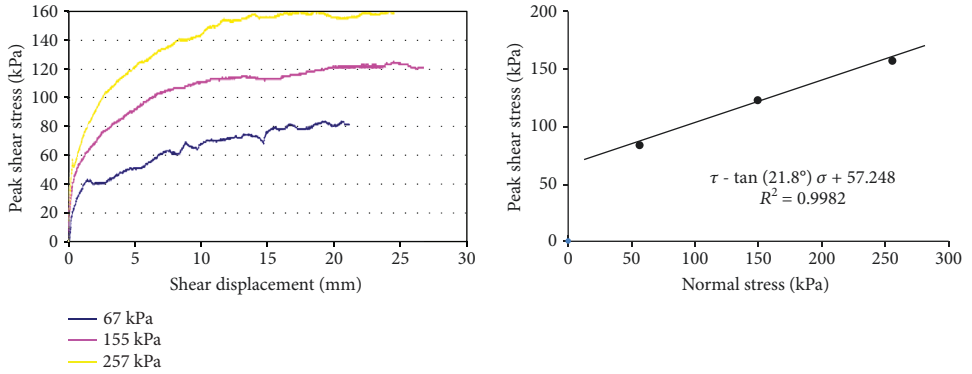

(d)

Figure 10: Continued.

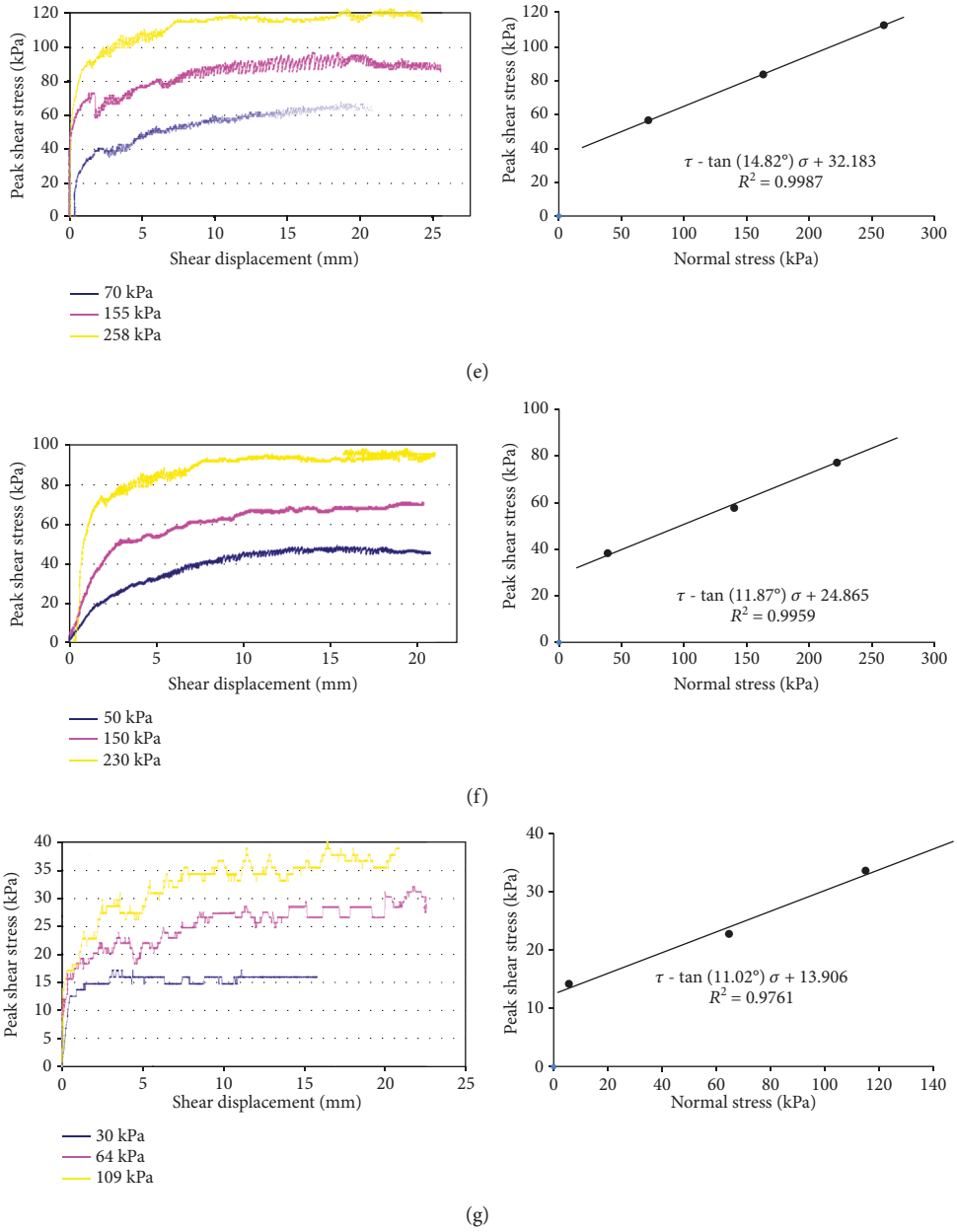

Figure 10: Medium-size direct shear test on remolded samples; shear stress-displacement curves and strength parameters of all seven groups.

Table 1: Direct shear tests parameters of soil with particle size less than 2 mm.

Group	Cohesion (kPa)	Angle of friction (°)	Average moisture content (%)
1	120	27.16	8.2
2	114.74	26.46	12
3	107.09	26.06	14.3
4	57.25	21.8	15.8
5	32.18	14.82	18.1
6	24.86	11.87	20
7	12.3	10.01	25

curves, the measured normal stress values were applied. There were six samples in the first group of tests; however, only four samples were remained effective. Four samples were used in the second group, and only three were proved to be effective. The normal stress of the tests was adjusted by manual pump control jack, and the horizontal shear force was applied through the electric pump drive jack with an average shear rate of 0.9 mm/min. The sample preparation process in the field is shown in Figure 12.

4.1. The First Group of Direct Shear Test. For the predefined 50 kPa normal stress test, the measured value of normal stress is 49 kPa and the maximum shear displacement is 56 mm. For the predefined 100 kPa normal stress test, the measured normal stress is 100 kPa, the maximum shear displacement

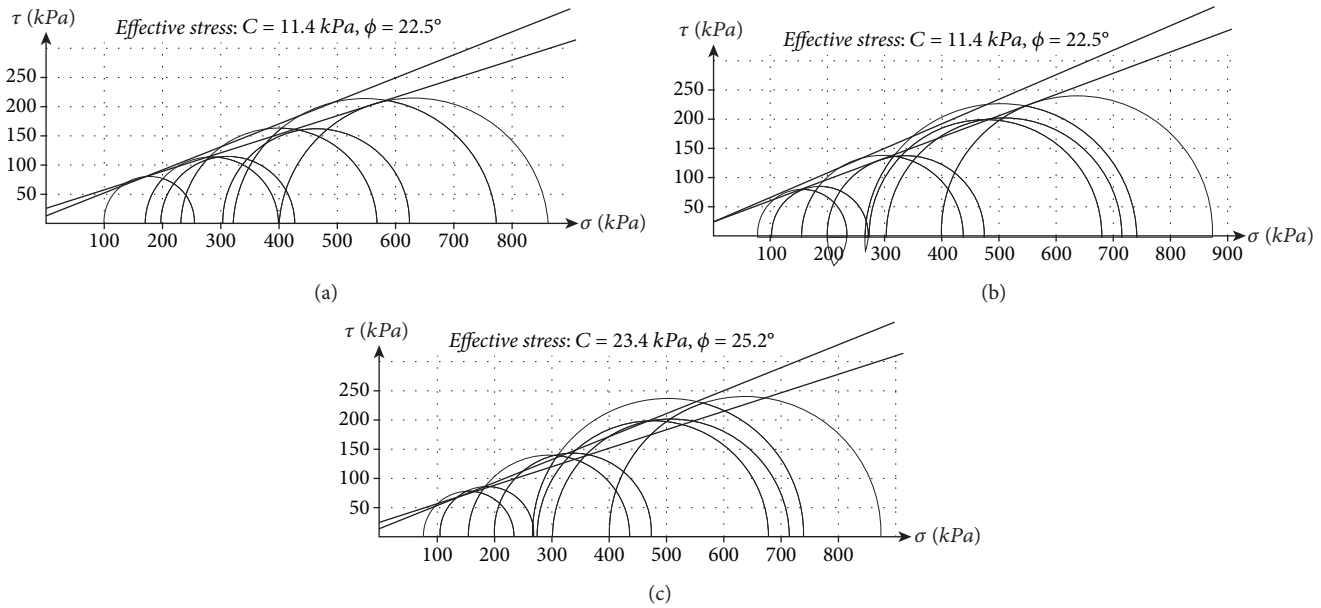

Figure 11: Tests fitting curve of soil samples for triaxial shear test (group a, b, and c).

Table 2: Results of triaxial consolidation undrained shear tests of soil samples.

$\sigma 3$	$\sigma 3'$	$\sigma 1$	$\sigma 1'$	$\frac{\sigma 1+\sigma 3}{2}$	$\frac{\sigma 1'+\sigma 3'}{2}$	$\frac{\sigma 1'-\sigma 3'}{2}$
Group A						
100	96.0	269.0	265.0	184.5	180.5	84.5
200	174.0	430.0	404.0	315.0	289.0	115.0
300	242.0	625.0	567.0	462.5	404.5	162.5
400	326.0	847.0	773.0	623.5	549.5	223.5
Group B						
100	68.5	271.0	239.5	185.5	154.0	85.5
200	159.5	474.0	433.5	337.0	296.5	137.0
300	173.5	708.0	681.5	501.0	477.5	204.0
400	266.0	872.0	738.0	636.0	502.0	236.0
Group C						
100	98.0	305.0	303.0	202.5	200.5	102.5
200	153.0	520.0	473.0	360.0	313.0	160.0
300	238.5	722.0	660.5	511.0	449.5	211.0
400	318.0	941.0	889.0	670.5	588.5	270.5

is 79 mm, and the average shear rate is 0.59 mm/min. For the 150 kPa normal stress test, the actual normal stress is 147 kPa, the maximum shear displacement is 85 mm, and the average shear speed is 1.3 mm/min; during the horizontal displacement of 0 mm to 1.32 mm, it failed to get the data due to the fault in the cable of horizontal shear stress sensor, but it did not make a great difference. For the predefined 200 kPa normal stress test, the measured value of normal stress is also 200 kPa and the maximum shear displacement is 85 mm. The results of the first group are good, and the shapes of the shear stress displacement curves are similar. After the peak, stress values keep steady. For the normal stress values of 49, 79, 174, and 200 kPa, the peak shear stress values are 50, 78, 110, and 137 kPa, respectively. The shear strength parameters in the form of cohesion and angle of friction are 21.17 kPa and 30.3°, respectively (Figure 13 and Table 3).

4.2. The Second Group of Direct Shear Test. During the test, it rained a lot which greatly influenced the results. There are only three effective samples in the second group of the test, and the measured values of normal stress are 98 kPa, 145 kPa, and 197 kPa. When the normal stress is 98 kPa, the maximum shear displacement is 86 mm and the average shear speed is 1.95 mm/min. When the normal stress is 145 kPa, the maximum shear displacement is 81 mm and the average shear speed is 1.75 mm/min. When the normal stress is 197 kPa, the maximum shear displacement is 83 mm and the average shear speed is 1.7 mm/min. The average shear speed of three samples is similar. When the displacement is about 40 mm, it reaches its peak, and then the value of stress keeps steady. For the normal stress values of 98, 145, and 197 kPa, the corresponding peak shear stress values are 82, 102, and 127 kPa, respectively. The results of the fitting curves are good, and the strength parameters in the form of cohesion and angle of friction are 37 kPa and 24.4°, respectively (Figure 14 and Table 3).

4.3. The In Situ Permeability Tests. Sixteen permeability tests were carried out in the Dasha landslide using the double-ring infiltration method using ASTM [21] D3385-09 (Figure 15(b)). During the test site preparation, the inner ring diameter of the infiltrometer was 25 cm while the outer ring diameter was 50 cm, and the height of the ring was 30 cm. During the experiment, the infiltrometer was dug into the soil at a depth of 10 cm keeping both rings concentric. Usually the bottom edge of the ring is not in well contact with the soils which lead to the leakage of water, resulting in a high permeability coefficient value. In order to reduce this error,

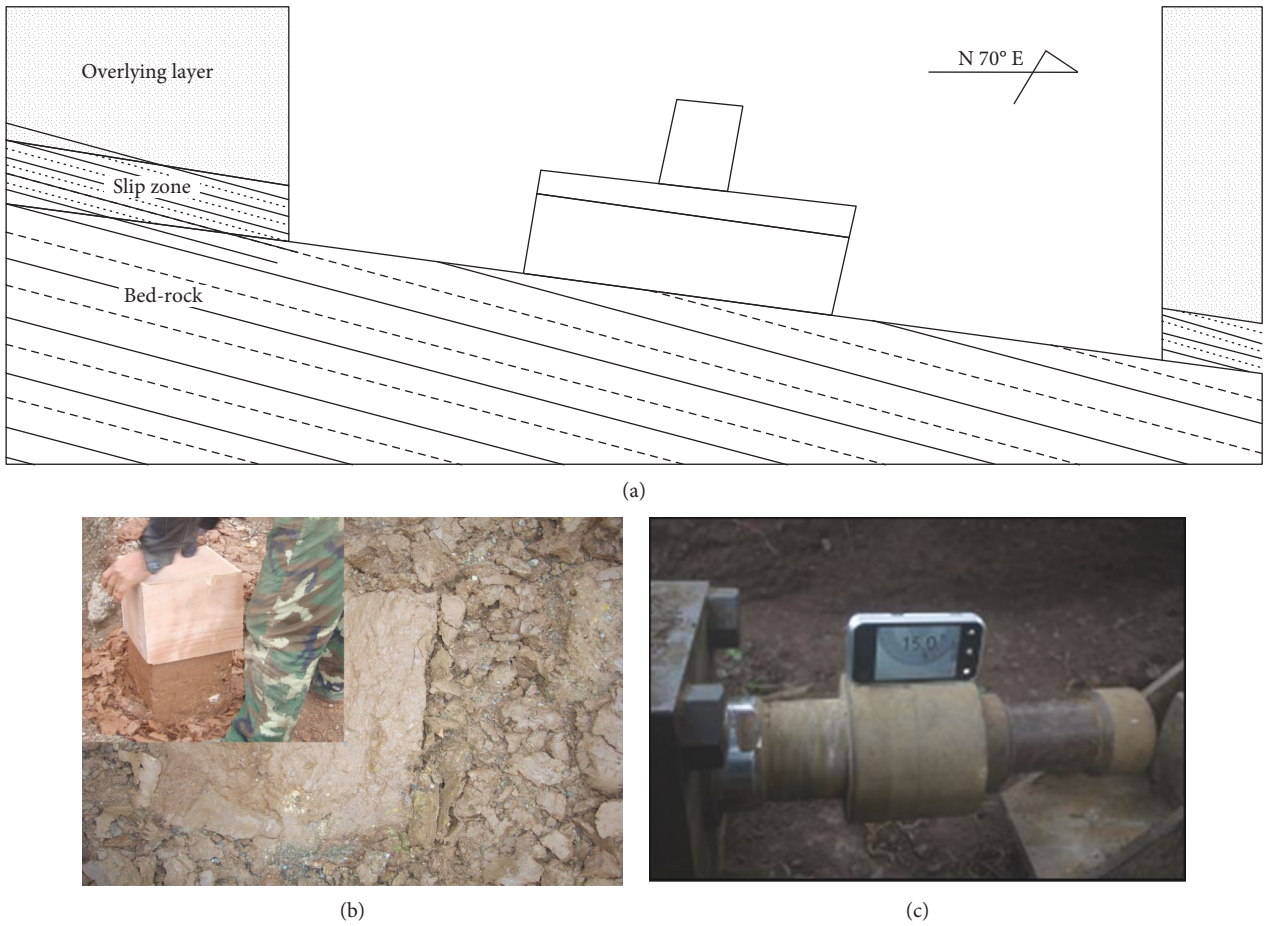

Figure 12: Sample preparation for test in field. (a) Schematic diagram of pruning samples, (b) inclined pruning samples, and (c) inclined push shear.

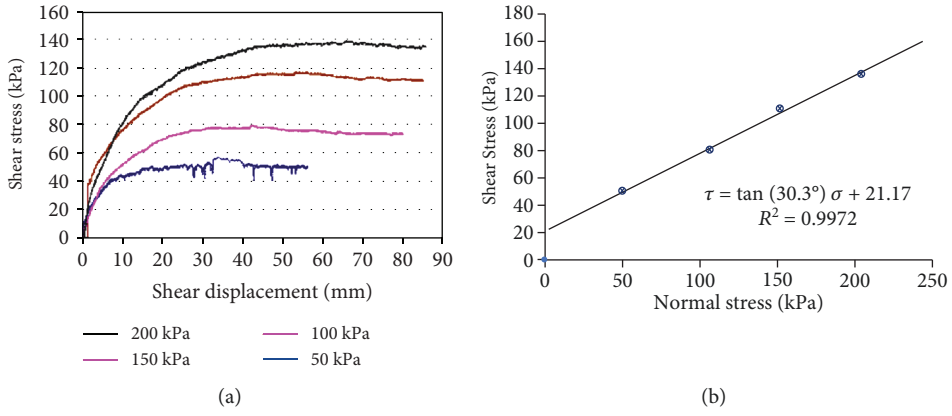

Figure 13: Shear stress-displacement curve and strength parameters of the first group.

firstly, the small trench was dug from top to bottom along the outer walls of both of the rings and then the bottom edge of the rings was sealed with bentonite, while the outer ring was filled with 10 cm thick compacted soil. The landslide has a gentle slope and is developed as farmland, so it is convenient while choosing test sites and water intake for in-site testing. Out of total sixteen permeability tests, the first four tests were carried within the area from where in situ direct shear tests were performed, while the rest of the test points were evenly distributed within the landslide body (Figure 15(a) and Table 3).

5. Stability Analysis

5.1. Three-Dimensional Stability Analysis Based on Strength Reduction Method. FLAC 3D software is used for stability analysis. The model area is 880 m × 900 m. X-axis which is parallel with the cross-section 1-1'of the landslide with the

Table 3: The test results of different parameters on site.

(a)

					Strength parameters	
First group of direct shear test of Dasha						
Normal stress (kPa)	49	100	147	200	Cohesion (kPa)	21.17
The peak shear stress (kPa)	50	78	110	137	Angle of friction (°)	30.3
Average moisture content of tests (%)	8.2	7.1	5.0	9.0		
Second group of direct shear test of Dasha						
Normal stress (kPa)	98	145	197	—	Cohesion (kPa)	37
The peak shear stress (kPa)	82	102	127	—	Angle of friction (°)	24.4
Average moisture content of tests (%)	6.9	7.1	7.5	—		

(b)

The permeability test in Dasha and in situ density		
The range of permeability (m/s)	The average permeability (m/s)	In situ density (g/cm^3)
4.530E-06…4.530E-05	2.11274E-05	2.233

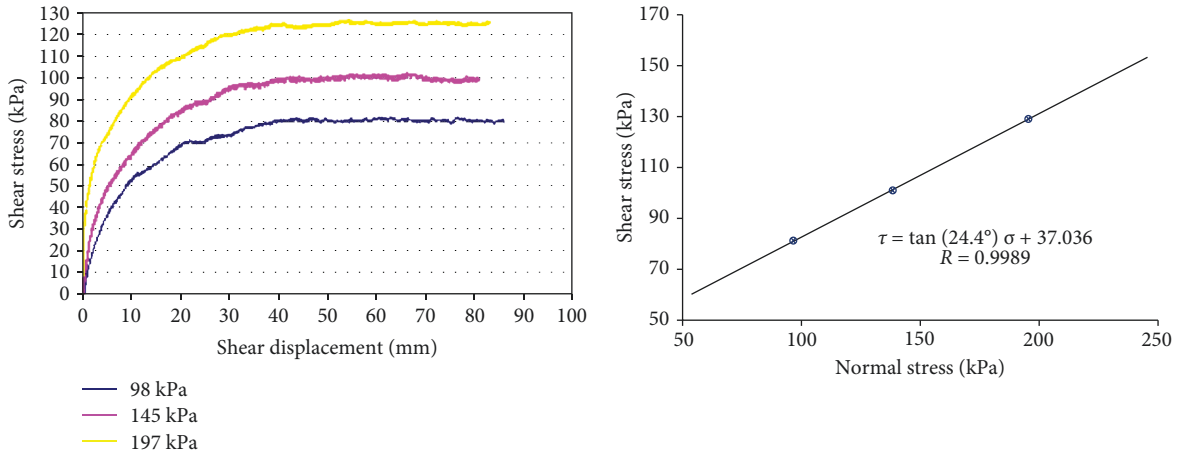

(a) (b)

Figure 14: Shear stress - displacement curve and strength parameters of second group.

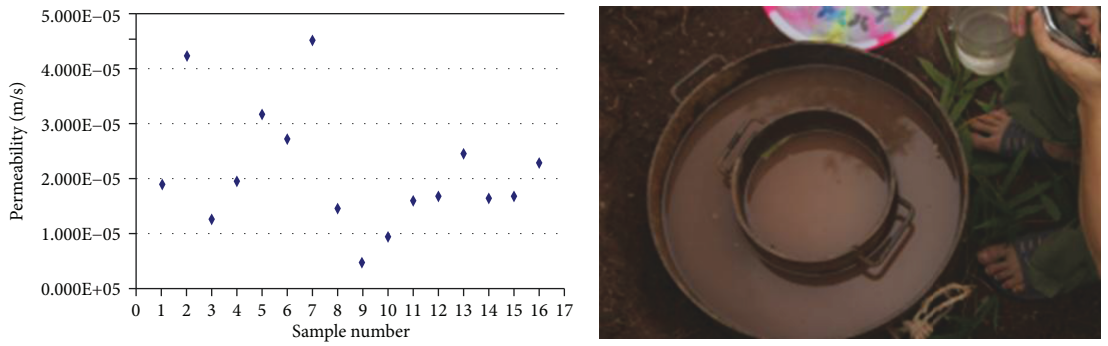

(a) (b)

Figure 15: (a) Distribution of in situ permeability tests; (b) permeability test in the field using the double-ring infiltrometer method.

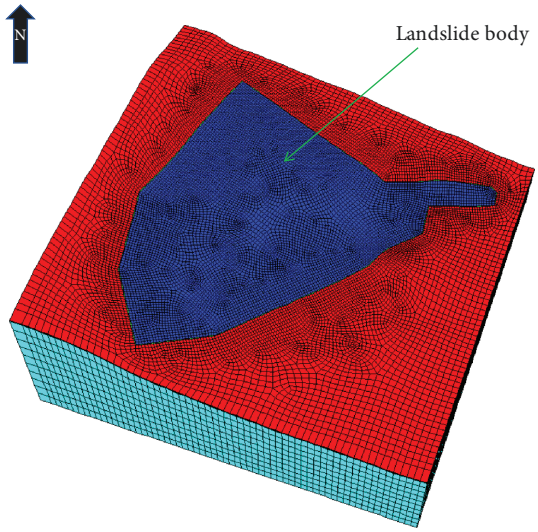

Figure 16: 3D numerical model of Dasha landslide.

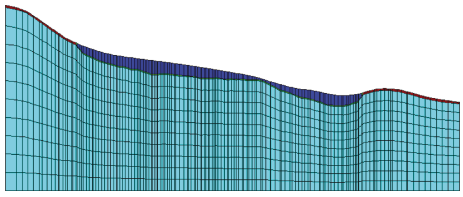

Figure 17: Sectional view of the model of Dasha landslide.

direction towards Jinsha River. Y-axis is vertical with respect to the cross-section 1-1' and the Z-axis with positive upward direction. The range of X-axis is 0~880 m, Y axis is 0~900 m, and Z-axis is from the elevation of 200 m up to the ground surface. Computational mesh is shown in Figures 16 and 17, and the model is divided into 182416 nodes and 166836 elements. In numerical analysis, the fixed constraints at the bottom of the model and normal constraints around the perimeter of the model were applied. X-axis is bounded by 0 m and 880 m, Y-axis is bounded by 0 m and 900 m, and Z-axis is bounded by 200 m. The slope materials were assumed to be perfectly elastoplastic and satisfy the Mohr-Coulomb failure criteria. Based on the actual geological and geomorphological conditions of the Dasha landslide, the numerical model was built which include the slip zone, the landslide, and the underlying bedrock. Three material layers were built including the slip zone, the landslide, and the bedrock. In order to obtain the geotechnical parameters of Dasha landslide, the in situ tests, as well as laboratory tests, were carried out. The parameters used in numerical modeling are shown in Table 4; bulk modulus (K) and shear modulus (E) were converted from Young's modulus (E) and Poisson' ratio (ν). The initial stress under the gravity and hydrostatic pressure were calculated under natural conditions.

The calculation is performed in two steps, while performing the calculations in natural condition (without considering water effect), the first step is to calculate elastic deformation and stress of bedrock, landslide body, and slip zone under the effect of gravity and as the initial state. The second step is to simulate the deformation development process by eliminating the initial elastic displacement and setting the slip zone as elastic-plastic. The slip zone was assumed as a perfect elastic-plastic constitutive model with yield criteria of Mohr-Coulomb, while the landslide body and the underlying bedrock were assumed as the linear elastic model. When considering the reservoir water level, the steady flow analysis is applied in this condition by assuming that the reservoir water level does not change and there is no raining. Analysis of transient flow is applied in other conditions. Water pressure change is measured by Abaqus software, and it can carry out coupled fluid-solid analysis in different conditions of rainfall and reservoir level and also export data of hydraulic condition and stress condition from analysis results as an initial state and finally import to the FLAC^{3D} landslide model for three-dimensional strength reduction analysis in the natural conditions (without considering the reservoir water level) to get the FOS of the landslide.

5.2. Three-Dimensional Strength Reduction Analysis without Consideration of Groundwater. Every strength reduction calculation is carried out by using the test of transfixion of slip plastic zone. Under the natural conditions without considering groundwater, the maximum principal stress distribution is shown in Figure 18 and the development process of slip plastic zone is shown in Figure 19. When the strength reduction factor (RF) reaches 1.212, it indicates that the continuous yield area has basically formed in the slip zone, with only a small range of area not reaching the yield limit, i.e., the factor of safety of the landslide is 1.212. The distribution and development of the slip plastic zone at the left side and the middle upper side enter the plastic phase earlier than the right side. The maximum principal stress of Dasha landslide within the range of the numerical simulation is about 8.0 MPa; the maximum principal stress of the slope is about 0.1 MPa. The principal stress values of the landslide range approximately from 0.4 MPa to 0.8 MPa. The maximum principal stress whose direction is nearly vertical is almost equal to the vertical stress.

5.3. Three-Dimensional Strength Reduction Analysis with Effect of Rainfall and Reservoir Filling. This condition is after the final phase of reservoir filling, which reflects the global stability of Dasha landslide with the consideration of the groundwater, reservoir level of 380 m, and rainfall conditions. For numerical simulation under the condition of heavy rainfall, the transient flow analysis is used. Under the condition of heavy rainfall, the changes of water pressures of Dasha landslide are shown in Figure 20. The figure shows that during heavy rainfall, the water pressures keep increasing gradually with the increase in rainfall, and the saturation line gradually increases as well. After the rain water pressure decreases, the saturation line gradually reduces to a particular reservoir level. The change of water pressures is not very significant after the rainfall. Under the condition of heavy rainfall of 94.7 mm in 2 hours, the factor of safety obtained by strength reduction method is 0.991, which does not meet the standards of safety requirements (Table 5).

Table 4: Calculation parameters of Dasha landslide taken from field and lab experiments.

Material	Unit weight (KN/m^3)		Elastic modulus (MPa)	Poisson's ratio	Natural		Saturated	
	Natural	Saturated			Cohesion (kPa)	Angle of friction (°)	Cohesion (kPa)	Angle of friction (°)
Landslide deposits	19	22	500	0.32	17	20	14	17
Slip zone	18	21	15	0.40	13	18	8	14
Bedrock	25	26	1000	0.28	1000	35	800	30

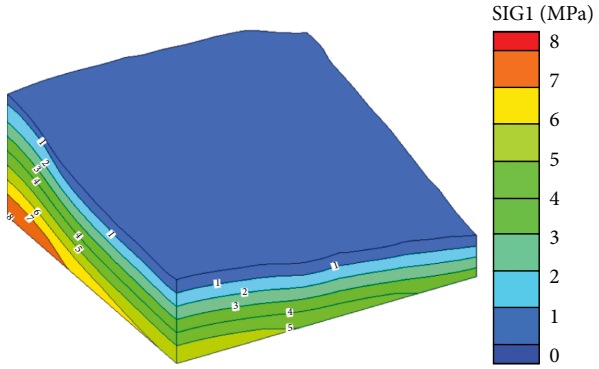

Figure 18: Maximum principal stress of Dasha landslide under the gravity.

6. Discussion

The Dasha landslide located at the right bank of the Jinsha River in the Xiangjiaba reservoir area has been studied from various aspects using diverse field, lab, and simulation techniques to better understand the slope stability in natural conditions as well as the effects of reservoir fluctuations on the slope stability. The stability, even the movement (e.g., [22]), of reactivated landslides has been successfully evaluated and interpreted using the assumption that shear strength mobilized on the slip surface of a landslide is equal to the residual shear strength on the basis of laboratory drained multiple reversal direct shear, or ring shear tests, independent of the time after reaching the residual condition. The landslides with a slip surface at residual condition rarely remain stationary for a long time and may move at the rate of approximately 2–50 mm/year (e.g., [22, 23]). The stability analysis and laboratory tests cannot be expected to yield results with accuracy better than approximately ±10% [24].

Skempton [24, 25] had done the benchmark studies on residual shear strength measured by laboratory tests, and it has been successfully used for stability analyses of reactivated landslides (e.g., [26, 27]; James 1970; [28–35]). The reversal direct shear tests or ring shear tests, using either undisturbed or reconstituted specimens, have become the most common methods for determining residual shear strength of stiff clays, shales, and mudstones (e.g., [29, 31, 36, 37]). For direct shear tests, the best procedure is to start with precut specimens, sometimes cut from intact undisturbed samples, but more often prepared from reconstituted samples [38].

Although each test has been discussed and explained with its results within the same section for better understanding of the readers, however, as there were numerous tests and their subgroups, so we tried to summarize the tests and compared with the previous studies as concluding section of the shear strength tests. As shown in Figure 8, the drained undisturbed sample test results for the peak shear strength and the residual shear strength in the form of frictional angle and cohesion are 26.18°, 18.88 kPa and 21.38°, 17.95 kPa, respectively. The average moisture content of the soil samples measured from shear surface after opening of the shear box is 17.0%. In the remolded direct shear tests, it was noted that the cohesion as well as the angle of internal friction decreases in all cases with a decrease in water content which shows the reliability of the tests (Figures 9 and 10). Both groups of the triaxial consolidation undrained shear tests show similar results; however, they show slight variations in strength parameters from the direct shear tests which is acceptable due to difference in the rest of the methods. For the in situ tests, two shear rates of 1.3 mm/minute and 1.75 mm/minute were applied in this study and the results show that the cohesion increases with shear rate while the angle of internal friction decreases [39].

The direct shear test results indicate that the residual strength of both in situ soils and disturbed soils from the slip zones of the Dasha landslide is influenced by their index properties, for example, the direct shear tests for the soil with less than 2 mm particle size; the strength parameters are greatly influenced by the moisture content, and with a decrease in moisture content, the values of the angle of friction and cohesion increases. However, influences of these index properties on residual strength are quite different for the in situ and disturbed soils. After the fourth cycle of shearing of the medium-sized reversal direct shear tests, the samples had basically reached the residual shear state. It was noted that the residual shear strength obtained by shear box tests has a nonzero cohesion component. Similar results were also reported by other researchers (e.g., [37, 40–43]). The simulation results show that the landslide is stable in the natural situation; however, the water fluctuation will lead to decrease the stability of the slope making it unstable.

7. Conclusions

The Dasha landslide was investigated in detail using field, land, and simulation methods to better understand the effects of reservoir water on the slopes along the banks of the Jinsha River in the Xiangjiaba reservoir. Based on our results and analysis, the following conclusions and recommendations can be drawn:

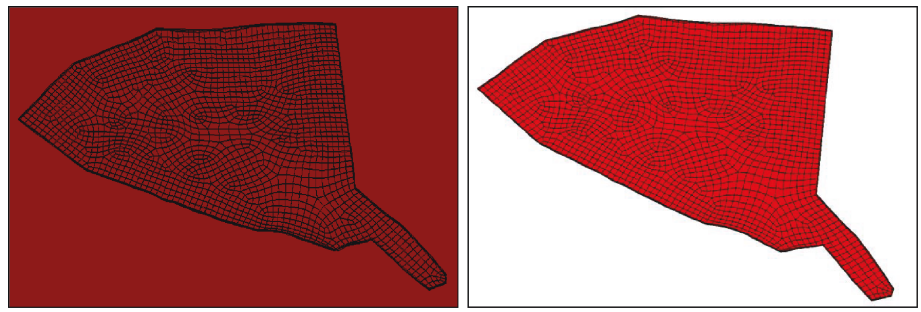

Figure 19: Plastic zone of Dasha landslide slip surface under the gravity.

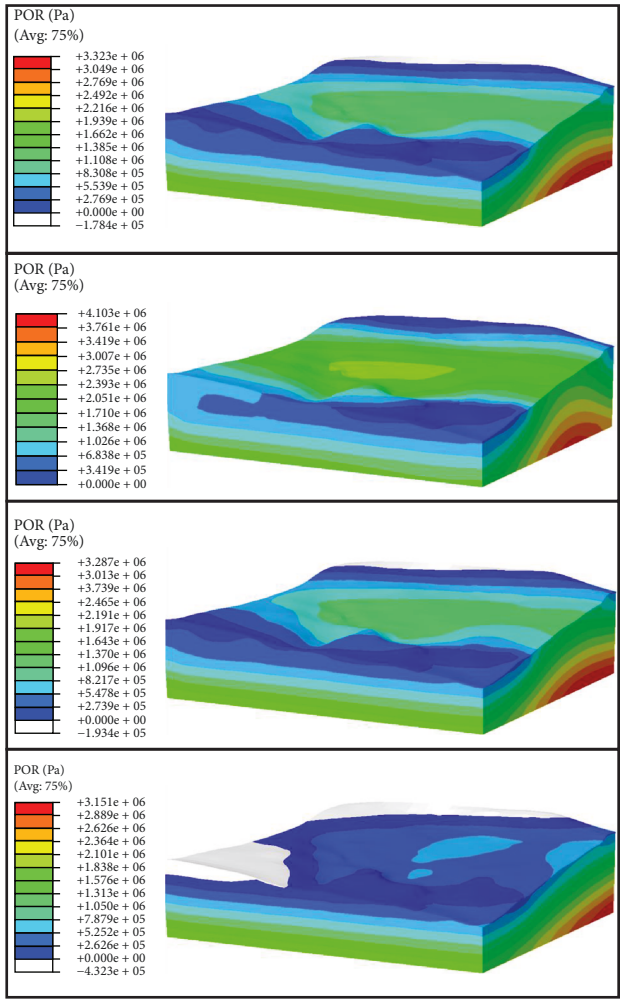

Figure 20: Distribution of water pressure of Dasha bank slope (rainfall in 2 hours is 94.7 mm).

Table 5: Factor of safety of Dasha landslide under different working conditions in different periods.

Period	Working condition	FOS using FLAC^{3D}
Construction	Natural	1.212
Operational	Fluctuation as designed, with effect of rainfall and rapid drawdown	0.991

(1) The underlying bedrock in the landslide area is composed of Suining Formation (silty mudstone interbedded with sandstone) of the Jurassic age. This landslide was reactivated during the rainy season in 1986, resulting in opening and cracking on the wall of houses and the ground surface

(2) The overall topography of Dasha landslide is relatively flat with an average slope angle of 15°; however, the back scarp and local terrain are relatively steep. The area of the landslide is about 29×10^4 m^2, and the maximum thickness of the landslide deposits revealed by drilling is about 40 m with the average thickness of about 20 m, and the volume is thus estimated being about 580×10^4 m^3

(3) A secondary landslide was also identified near the toe with an area of about 2.7×10^4 m^2, with an average thickness of about 6 m and an estimated volume of about 16×10^4 m^3

(4) The factor of safety (FOS) of Dasha landslide obtained by 3D strength reduction cannot meet the minimum safety requirement under the working condition of reservoir level fluctuation as designed, due to the effect of rainfall and rapid drawdown. For the safety of local residents, it is recommended that surface monitoring should be carried out so that early warning can be issued prior to failure

(5) The bedding landslides of red stratum in the Xiangjiaba reservoir area (for example, Dasha landslide) are characterized by slow moving. The shear rate effect of the slip surface should be carried out using ring shear apparatus where possible. This would be useful to predict the deformation of active landslides

(6) Comprehensive monitoring, including rainfall, reservoir level fluctuation, groundwater level, surface displacement, and horizontal displacements at different depths, should be conducted on active landslides so that early warning can be issued and local residents can be evacuated prior to failure. In addition, these monitoring data can be very useful for quantitative evaluation of effect of rainfall as well as the reservoir level fluctuation in landslide activation and reactivation in the reservoir areas

Data Availability

The data used to support the findings of this study are available from the corresponding author upon request.

Disclosure

The earlier version of the abstract was published in a conference of the World Academy of Science, Engineering and Technology International Journal of Geological and Environmental Engineering Vol: 12, No: 6, 2018.

Conflicts of Interest

The authors declare that they have no conflicts of interest.

Acknowledgments

This research is financially supported by the Chinese Academy of Sciences President's International Fellowship Initiative (Grant No. 2018PC0009) and the Institute of Geology and Geophysics partial fellowship grant. Help from faculty and staff of the Institute of Rock and Soil Mechanics, Chinese Academy of Sciences, Wuhan, China, is really appreciated.

References

[1] ICOLD (International Commission of Large Dams), *Reservoir Landslides: Investigation and Management—Guidelines and Case Histories*, International Commission of Large Dams Publications, 124, Paris, 2002.

[2] W. Riemer, "Landslides and reservoirs (keynote paper)," in *Proceedings of the 6th International Symposium on Landslides*, pp. 1373–2004, Christchurch, 1992.

[3] J. H. Deng, S. S. Ma, and C. F. Lee, "Reactivation of a reservoir landslide," in *Proceedings of the 1st International Conference on Slope Engineering*, pp. 930–935, Hong Kong, December 2003.

[4] X. Z. Guo, *Geological Hazards of China and their Prevention and Control*, Geological Publication House, Beijing, 1991.

[5] X. M. Hu, "The study on the slope stability near the dam of Chenchun Reservoir," *Acta Scientiarum Naturalium Universitatis Pekinensis*, vol. 35, no. 6, pp. 809–815, 1999.

[6] G. Y. Li, *The research on stability of Jinlongshan landslide after the reservoir storing water, [M.S. thesis]*, Chengdu University of Technology, 2002.

[7] H. Liu, R. G. Deng, and Z. Y. Zhang, "Characteristics and genetic analysis of the landslides along Baozhusi reservoir bank in Sichuan," *The Chinese Journal of Geological Hazard and Control*, vol. 12, no. 4, pp. 48–52, 2001.

[8] H. Peng, S. F. Chen, and S. H. Chen, "Analysis on unsaturated seepage and optimization of seepage control for Dayantang landslide in Shuibuya project," *Chinese Journal of Rock Mechanics and Engineering*, vol. 21, no. 7, pp. 1027–1033, 2002.

[9] Y. H. Wei, *The research on the stability of the reservoir bank in Fengjie section of the Three Gorges Reservoir, the Yangtze River, [M.S. thesis]*, Chengdu University of Technology, 2002.

[10] Q. W. Wu and C. H. Wang, "The largest landslide of half-rock and half-soil in China," *Typical slopes in China*, pp. 225–230, Science Press, Beijing, 1988.

[11] L. Xu, *A study on genetic mechanism and stability of Jinjiang landslide at the Baihetan hydropower station in the Jinsha River, [M.S. thesis]*, Chengdu University of Technology, 2004.

[12] R. F. Yu, "Studies on landslide induced waves and landslide warning system near Longyangxia hydroelectric power station in Yellow River," *Water Power*, no. 3, pp. 14–17, 1995.

[13] L. X. Zhong, "Case study on significant geo-hazards in China," *The Chinese Journal of Geological Hazard and Control*, vol. 10, no. 3, pp. 1–10, 1999.

[14] J. Iqbal, D. Fuchu, and X. Tu, "Landslide hazards in reservoir areas: case study of Xiangjiaba reservoir, Southwest China," *Natural Hazards Review*, vol. 18, no. 4, 2017.

[15] J. Iqbal, F. Dai, M. Hong, and X. Tu, "Failure mechanism and stability analysis of an active landslide in the Xiangjiaba reservoir area, Southwest China," *Journal of Earth Science*, vol. 29, no. 3, pp. 646–661, 2018.

[16] L. Xu, F. C. Dai, J. Chen, J. Iqbal, and Y. Qu, "Analysis of a progressive slope failure in the Xiangjiaba reservoir area, Southwest China," *Landslides*, vol. 11, no. 1, pp. 55–66, 2014.

[17] B. Huang, Y. Yin, S. Wang, G. Liu, and J. Tan, "Tangjiaxi landslide and impulse wave analysis in Zhexi reservoir of China by granular flow coupling model," *Natural Hazards and Earth System Sciences Discussions*, vol. 17, pp. 657–670, 2017.

[18] A. Panizzo, P. De Girolamo, M. Di Risio, A. Maistri, and A. Petaccia, "Great landslide events in Italian artificial reservoirs," *Natural Hazards and Earth System Sciences*, vol. 5, no. 5, pp. 733–740, 2005.

[19] M. Yamao, R. C. Sidle, T. Gomi, and F. Imaizumi, "Characteristics of landslides in unwelded pyroclastic flow deposits, southern Kyushu, Japan," *Natural Hazards and Earth System Sciences*, vol. 16, no. 2, pp. 617–627, 2016.

[20] Y. Yonghui, Z. Baiping, M. Xiaoding, and M. Peng, "Large-scale hydroelectric projects and mountain development on the upper Yangtze River," *Mountain Research and Development*, vol. 26, no. 2, pp. 109–114, 2006.

[21] ASTM, *D3385-09, Standard Test Method for Infiltration Rate of Soils in Field Using Double-Ring Infiltrometer*, ASTM International, West Conshohocken, PA, USA, 2009.

[22] A. W. Skempton, A. D. Leadbeater, and R. J. Chandler, "The Mam Tor landslide North Derbyshire," *Philosophical Transactions of the Royal Society A: Mathematical, Physical and Engineering Sciences*, vol. 329, no. 1607, pp. 503–547, 1989.

[23] A. W. Skempton and J. N. Hutchinson, "Stability of natural slopes and embankment foundations," in *Proceedings of the 7th International Conference on Soil Mechanics and Foundation Engineering, 3(State of the Art), Sociedad Mexicana de Mecanica de Suelos*, pp. 291–340, Mexico City, Mexico, 1969.

[24] A. W. Skempton, "Residual strength of clays in landslides, folded strata and the laboratory," *Geotechnique*, vol. 35, no. 1, pp. 3–18, 1985.

[25] A. W. Skempton, "Long-term stability of clay slopes," *Geotechnique*, vol. 14, no. 2, pp. 77–102, 1964.

[26] J. N. Hutchinson, "A reconsideration of the coastal landslides at Folkestone Warren, Kent," *Géotechnique*, vol. 19, no. 1, pp. 6–38, 1969.

[27] A. W. Skempton and D. J. Petley, "The strength along structural discontinuities in stiff clays," in *Proceedings of the Geotechnology Conference on Shear Strength Properties of Natural Soils and Rocks, NGI, Norwegian Geotechnical Institute*, vol. 2, pp. 29–47, Oslo, Norway, 1967.

[28] F. Blondeau and H. Josseaume, "Mesure de la resistance au asaillement rediduelle en laboratoire," *Bulletin de liaison des laboratoires des ponts et chaussées*, pp. 90–106, 1976, Numero Special II.

[29] E. N. Bromhead and N. Dixon, "The field residual strength of London Clay and its correlation with loboratory measurements, especially ring shear tests," *Géotechnique*, vol. 36, no. 3, pp. 449–452, 1986.

[30] R. J. Chandler, "A Discussion on valley slopes and cliffs in southern England: morphology, mechanics and Quaternary history - The history and stability of two Lias clay slopes in the upper Gwash valley, Rutland," *Philosophical Transactions of the Royal Society of London, Series A*, vol. 283, no. 1315, pp. 463–491, 1976.

[31] R. J. Chandler, "Back analysis techniques for slope stabilization works: a case record," *Géotechnique*, vol. 27, no. 4, pp. 479–495, 1977.

[32] R. J. Chandler, "Recent European experience of landslides in overconsolidated clays and soft rocks," in *Proceedings of the 4th International Symposium on Landslides, Canadian Geotechnical Society*, vol. 1, pp. 61–81, Richmond, BC, Canada, 1984.

[33] N. R. Morgenstern, "Slopes and excavations," in *9th International Conference on Soil Mechanics and Foundation Engineering, 12 (State of the Art)*, pp. 567–581, 1977.

[34] D. J. Palladino and R. B. Peck, "Slope failures in an overconsolidated clay, Seattle, Washington," *Géotechnique*, vol. 22, no. 4, pp. 563–595, 1972.

[35] K. Terzaghi, R. B. Peck, and G. Mesri, *Soil Mechanics in Engineering Practice*, Wiley, New York, 3rd Ed edition, 1996.

[36] A. W. Bishop, G. E. Green, V. K. Garga, A. Andresen, and J. D. Brown, "A new ring shear apparatus and its application to the measurement of residual strength," *Géotechnique*, vol. 21, no. 4, pp. 273–328, 1971.

[37] T. D. Stark and H. T. Eid, "Drained residual strength of cohesive of soils," *Journal of Geotechnical Engineering*, vol. 120, no. 5, pp. 856–871, 1994.

[38] G. Mesri and F. Cepeda-Diaz, "Residual shear strength of clays and shales," *Géotechnique*, vol. 36, no. 2, pp. 269–274, 1986.

[39] R. Saito, H. Fukuoka, and K. Sassa, "Experimental study on the rate effect on the shear strength," in *Disaster Mitigation of Debris Flows, Slope Failures and Landslides*, pp. 421–427, Universal Academy Press, Inc., Tokyo Japan, 2006.

[40] H. Rahardjo, K. K. Aung, E. C. Leong, and R. B. Rezaur, "Characteristics of residual soils in Singapore as formed by weathering," *Engineering Geology*, vol. 73, no. 1-2, pp. 157–169, 2004.

[41] A. Rouaiguia, "Residual shear strength of clay-structure interfaces," *International Journal of Civil& Environmental Engineering*, vol. 10, pp. 6–18, 2010.

[42] B. P. Wen, A. Aydin, N. S. Duzgoren-Aydin, Y. R. Li, H. Y. Chen, and S. D. Xiao, "Residual strength of slip zones of large landslides in the Three Gorges area, China," *Engineering Geology*, vol. 93, no. 3-4, pp. 82–98, 2007.

[43] C. Xu, X. Xu, F. Dai, and A. Saraf, "Comparison of different models for susceptibility mapping of earthquake triggered landslides related with the 2008 Wenchuan earthquake in China," *Computers & Geosciences*, vol. 46, pp. 317–329, 2012.